The Cu-Se (Copper-Selenium) System

63.546 amu 78.96 amu

By D. J. Chakrabarti and D. E. Laughlin
Carnegie-Mellon University

Equilibrium Diagram

The equilibrium phases at one atmosphere displayed in Fig. 1 are (1) the liquid, L, that manifests two miscibility gaps, namely (*a*) at copper-rich compositions, between the liquids L_1 and L_2 above 1100 °C, and (*b*) at selenium-rich compositions, between the liquids L_2 and L_3 above 523 °C; (2) the face-centered cubic terminal solid solution based on Cu, with restricted solubility of Se amounting to 0.009 at.% at 900 °C; (3) the rhombohedral terminal solid solution based on Se with presumably negligible solubility of Cu; (4) the monoclinic Cu_2Se compound (αCu_2Se), stable up to 123 ± 15 °C; (5) the face-centered cubic high-temperature modification of Cu_2Se ($\beta Cu_{2-x}Se$), stable between 123 ± 15 and 1130 °C at stoichiometry ($x = 0$) and with a broad homogeneity range extended on the Se side to form a defect compound (see Fig. 2); (6) the tetragonal stoichiometric compound Cu_3Se_2, stable up to 112 °C; (7) the hexagonal stoichiometric compound CuSe (αCuSe), stable up to 51 °C; (8) the orthorhombic modification of the CuSe compound (βCuSe), stable between 51 and 120 °C; (9) the hexagonal high-temperature modification of the Cu-Se compound (γCuSe), stable between 120 and 377 °C; and (10) the orthorhombic stoichiometric compound $CuSe_2$, stable up to 332 °C.

The chalcogenides exhibit various properties that are of considerable theoretical and practical importance. The study of chalcogenides, in particular, of the IB metals, has been of considerable interest. The wide variety of property manifested by these classes of materials is evident in the Cu-Se system, where one of the compounds, cuprous selenide containing excess Se, $Cu_{2-x}Se$, is a *p*-type extrinsic semiconductor, and the dichalcogenide, $CuSe_2$, is a superconductor at low temperatures.

At least three of the compounds in the Cu-Se system occur as minerals in nature and have been the object of study in different disciplines. These are the minerals berzelianite, $Cu_{2-x}Se$, umangite, Cu_3Se_2, and klockmannite, αCuSe. The fourth naturally occurring mineral, athabaskite (Cu_5Se_4), has so far eluded synthesis in the laboratory and does not apparently exist as an equilibrium phase in this system.

Earlier work covering the copper side of the diagram at high temperature is reviewed by [Hansen]. Subsequent to this, extensive studies have been carried out by Heyding [1] and by Murray and Heyding [2] extending from 27 to 70 at.% Se as a function of temperature to 880 °C and pressure to 50 kbar, using differential thermal analysis (DTA) and both room temperature and high temperature X-ray diffraction methods. Studies over a wide range of temperature and composition, using DTA, X-ray, microscopy and microhardness techniques, were also carried out by Babitsyna *et al.* [3]. Furthermore, phase boundary determinations in the solid state by DTA and in the liquid state by isothermal holding of the melt under inert gas were carried out by Bernardini *et al.* [4, 5] and by Burylev *et al.* [6], respectively. Homogeneity range for a portion of the diagram below room temperature was determined by Ogorelec *et al.* [7] by means of electrical conductivity measurement.

There is qualitative agreement among these works except for the occurrence of the compound $CuSe_2$, which

Fig. 1 Cu-Se Phase Diagram

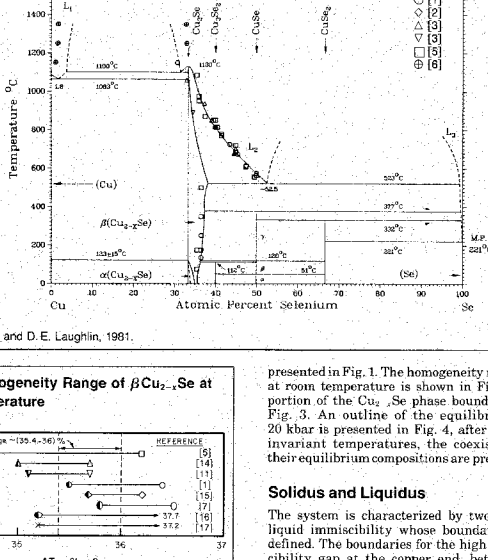

D.J. Chakrabarti and D.E. Laughlin, 1981.

Fig. 2 Homogeneity Range of $\beta Cu_{2-x}Se$ at Room Temperature

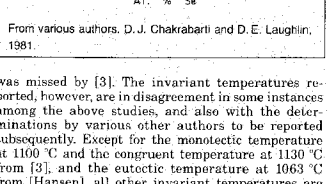

From various authors. D.J. Chakrabarti and D.E. Laughlin, 1981.

was missed by [3]. The invariant temperatures reported, however, are in disagreement in some instances among the above studies, and also with the determinations by various other authors to be reported subsequently. Except for the monotectic temperature at 1100 °C and the congruent temperature at 1130 °C from [3], and the eutectic temperature at 1063 °C from [Hansen], all other invariant temperatures are accepted from [2] for drawing the phase diagram, in view of the reported precision in measurements and better consistency with other published works. The temperatures reported by [2] are often lower than the other reported values.

The provisionally evaluated equilibrium phase diagram for the Cu-Se system under one atmosphere is presented in Fig. 1. The homogeneity range of $\beta Cu_{2-x}Se$ at room temperature is shown in Fig. 2; an enlarged portion of the $Cu_{2-x}Se$ phase boundaries is shown in Fig. 3. An outline of the equilibrium diagram at 20 kbar is presented in Fig. 4, after [2]. The accepted invariant temperatures, the coexisting phases and their equilibrium compositions are presented in Table 1.

Solidus and Liquidus

The system is characterized by two large regions of liquid immiscibility whose boundaries are not well defined. The boundaries for the high temperature miscibility gap at the copper end, between the liquids L_1 and L_2, were determined by [6] by isothermal holding of the melt under argon followed by rapid quenching and subsequent chemical analysis of the solidified sections. These data, plotted in Fig. 1, suggest a high critical temperature, in excess of 1500 °C.

The monotectic temperature at 1100 °C determined by [3], by thermal analysis on alloys made from high purity materials, is accepted. The only other quoted value is 1107 °C given by [Hansen], which is an average between 1104 and 1109 °C reported from very early works. The only available data on the eutectic temperature and composition come from [Hansen]. Assuming a negligible solubility of Se in Cu at the eutectic temperature at 1063 °C and applying the Clausius/Clapeyron approximation, the reported eutectic composition is within 0.1 at.% of the calculated value. Thus, the composition–temperature data appear to be self-consistent and are accepted as such. The congruent melting point of Cu_2S is reported to be 1130 °C by [3], 1148 ± 5 °C by [8] and 1113 °C by [9]. The result from

Fig. 3 Enlarged Portion of $Cu_{2-x}Se$ Phase Boundaries at Low Temperatures

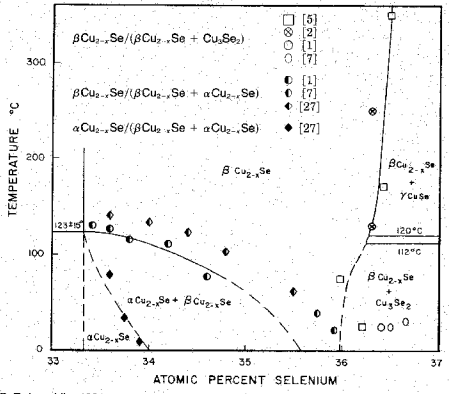

D. J. Chakrabarti and D. E. Laughlin, 1981.

[3] is accepted because of the use of well-defined experimental procedures and of high purity material.

The occurrence of the second miscibility gap between L_1 and L_2 is confirmed by [3], who observed two layers in the melt above 50 at.% Se. Data defining the boundaries are lacking. The accepted monotectic temperature is 523 °C, according to [2]. The other values reported are 523 °C [1], 540 °C [3] and 523 °C [5], all based on thermal analysis, the last one referring to both heating and cooling cycles.

The $L/(L + \beta Cu_{2-x}Se)$ liquidus boundary has been determined by [1], [3] and [5]. The DTA results, in particular those of [1] and [3] as read out from their figures and plotted in Fig. 1, are in good agreement with one another. The extrapolation of this boundary line to the 523 °C invariant represents the monotectic composition of the liquid L_2 at 52.5 at.% Se. This composition is outside the range of 50 to ~52 at.% Se suggested by [5], whose thermal data indicated considerable scatter including an abrupt deviation at low temperatures. Therefore, the composition of L_2 at the monotectic point is taken at ~52.5 at.% Se, whereas that for L_1 is not determined.

Terminal Solid Solutions

The solubility of Se in Cu is very restricted, that is, reported to be considerably below 0.02 at.% at temperatures up to 800 °C [Hansen]. More accurate determinations were made in recent times by Tayler *et al.* [12] and earlier by Smart and Smith [13] from electrical resistivity measurements. The two results shown in Table 2 are in fair agreement with each other below

Fig. 4 Cu-Se Phase Diagram at 20 kbar

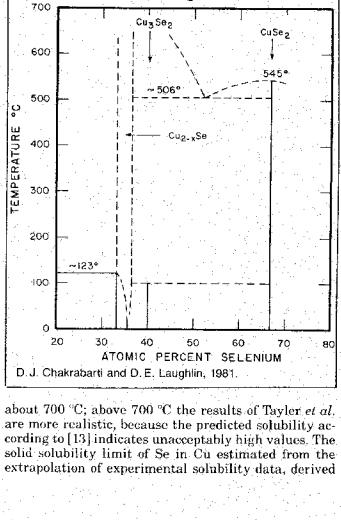

D. J. Chakrabarti and D. E. Laughlin, 1981.

about 700 °C; above 700 °C the results of Tayler *et al.* are more realistic, because the predicted solubility according to [13] indicates unacceptably high values. The solid solubility limit of Se in Cu estimated from the extrapolation of experimental solubility data, derived

Table 1 Temperatures and Compositions of Reactions in the Cu-Se System

Reaction	Phases	Composition, at.% Se	Temperature (a), °C, from reference [1]	[2]	[3]	[5]	[9]	Other
Congruent	βCu_2Se, L_2	33.3, 33.3	···	···	**1130**	···	1113	1148[6]
Monotectic	L_1, L_2, $\beta Cu_{2-x}Se$	···, ···, ~33.3	···	···	**1100**	···	···	1107[Hansen]
Eutectic	(Cu), L_1, $\beta Cu_{2-x}Se$	>99.9, ~1.8, ~33.3	···	···	···	···	1068	**1063**[Hansen]
Peritectoid	$\beta Cu_{2-x}Se$, $\alpha Cu_{2-x}Se$, (Cu)	~33.3, ~33.3, ~0	131	**123**	162	138	···	···
Monotectic	$\beta Cu_{2-x}Se$, L_2, L_3	~36.5, ~52.5, ···	523	**523**	540	523	···	···
Peritectic	$\beta Cu_{2-x}Se$, $\gamma CuSe$, L_3	~36.5, 50, ···	382	**377**	400	384	···	···
Peritectic	$\gamma CuSe$, $CuSe_2$, L_3	50, 66.7, ···	342	**332**	···	343	···	···
Eutectic/peritectic	$CuSe_2$, (Se), L_3	66.7, ~100, ···	218	218	···	226	···	**221**[10]
Eutectoid/peritectoid	$\gamma CuSe$, $\beta CuSe$, $CuSe_2$	~50, ~50, 66.7	···	**~120(b)**	···	···	···	120[11]
Eutectoid/peritectoid	$\gamma CuSe$, $\beta CuSe$, $\beta Cu_{2-x}Se$	~50, ~50, ~36.5	···	**~120(b)**	···	···	···	···
Peritectoid	$\beta Cu_{2-x}Se$, Cu_2Se_2, $\beta CuSe$	~36.5, 40, 50	135	112	175	143	···	···
Eutectoid/peritectoid	$\beta CuSe$, $\alpha CuSe$, $CuSe_2$	~50, ~50, 66.7	53	**~51(c)**	80	60	···	···
Eutectoid/peritectoid	$\beta CuSe$, $\alpha CuSe$, Cu_2Se_2	~50, ~50, 40	···	**~51(c)**	···	···	···	···

(a) Accepted temperatures are shown in boldface type. (b) Temperatures are close but not equal to each other. (c) Temperatures are close but not equal to each other.

Table 2 Solid Solubility of Se in Cu

Temperature, °C	Composition, at.% Se from reference [12]	[13]
590	0.0003(a)	0.0005
609	0.0010(a)	0.0010
675	0.0020	···
700	···	0.0021
735	0.0034	···
800	0.0053	0.0120
845	0.0068	···
900	0.0092	···
950	0.0120(a)	···
1000	0.0154(a)	···
1050	0.0183(a)	···
1063	~0.021	···

(a) Values extrapolated from experimental results.

Table 3 Homogeneity Range of $\beta Cu_{2-x}Se$ at Room Temperature

Reference	Composition range x	at.% Se	Comment
[1]	0.18 to 0.25	35.5 to 36.4	a
[5]	0.11 to 0.24	34.6 to 36.2	a
[7]	0.21 to 0.26	~35.8 to ~36.5	b
[11]	0.15 to 0.20	35.1 to 35.7	a
[14]	0.14 to 0.19	35.0 to 35.6	a
[15]	0.20 to 0.24	35.7 to 36.2	a
[16]	0.18 to 0.31	35.5 to 37.2	a
[17]	0.16 to 0.35	35.2 to 37.7	c

(a) From DTA and X-ray measurements on thermally prepared sample. (b) From electrical conductivity measurement. (c) For electrolytically prepared sample.

from the measurements of residual resistivity (at liquid helium temperature) by [12], is ~0.021 at.% Se at 1063 °C. No data are available for the solubility of Cu in Se.

Intermediate Phases

The system is characterized by the occurrence of a number of compounds. Except for one, all appear to be stoichiometric in composition, with negligible homogeneity range.

Cu_2Se/$Cu_{2-x}Se$ High-Temperature Phase. The Cu_2Se compound is involved at high temperatures in three different reactions: (*a*) congruent at 1130 °C [3], (*b*) monotectic at 1100 °C [3], and (*c*) eutectic transformation at 1063 °C [Hansen]. It goes through a polymorphic transformation at low temperature. The homogeneity range of Cu_2Se extends to higher selenium concentrations forming the copper-deficient $Cu_{2-x}Se$ phase. $Cu_{2-x}Se$ is stable at room temperature within narrow composition limits. The results from the different studies are shown in Table 3 and Fig. 2. Based on these figures, the homogeneity range of $Cu_{2-x}Se$ at room temperature is taken approximately between 35.4 and 36.0 at.% Se, corresponding to $0.18 < x < 0.22$.

The homogeneity range of $Cu_{2-x}Se$ phase increases further at higher temperatures. The width of the phase field from 75 to 500 °C was determined by [2] and [5] from the break of the lattice parameter values at the phase boundaries at each temperature. The results plotted in Fig. 1 show an almost vertical phase boundary on the Se side with a probable positive slope near room temperature [2]. Lorenz and Wagner [18] observed an extension of the $Cu_{2-x}Se$ phase field to Cu/Se ratio less than 1.86 (i.e., >35 at.% Se) at 400 °C by coulometric titration. Borchert [19] proposed the resultant structure as deficient in Cu atoms with the boundary at 20 °C at about 35.7 at.% Se ($x = 0.20$). Early [20] confirmed the defect structure, but suggested the extension of the field up to 35.1 at.% Se ($x = 0.15$). One of the earliest structure studies is reported by Rahlfs [21].

The composition of the copper-rich boundary of $\beta Cu_{2-x}Se$ at 400 °C estimated from the coulometric titration is $Cu_{1.9975}Se$ by [18] and $Cu_{1.9980}Se$ by [22]. The coulometric titration (300 to 420 °C) and thermal emf measurements (300 to 600 °C) of Konev *et al.* [23] indicate that, below about 600 °C, the composition of Cu_2Se deviates from stoichiometry toward higher Se levels whose magnitude increases progressively with the reduction in temperature. According to the studies between 0 and 200 °C by Migatanai *et al.* [24], similar deviation from stoichiometry also exists with the lower temperature modification (α) of $Cu_{2-x}Se$. These studies suggest that below 600 °C the (Cu) phase is in equilibrium with $Cu_{2-x}Se$ phase, where $x > 0$, and contradict the reported occurrence of $Cu_{2-x}Se$ at 110 °C in the presence of excess Cu [11].

In contrast, several studies by thermal and electrical methods [1, 7, 11] show that the deviation from the stoichiometric Cu_2Se composition on the copper-rich side does not start until about 130 °C. Because the reported magnitude of deviation from the stoichiometry between 600 and 200 °C is very small, it is difficult to resolve the discrepancy between the two sets of observations. Tentatively, the temperature denoted by the latter studies is accepted and indicated in Fig. 3.

The $\alpha \rightarrow \beta$ polymorphic transformation temperature for the $Cu_2Se/Cu_{2-x}Se$ phase has been determined by X-ray, DTA, electrical conductivity and thermoelectric power techniques. The results presented in Table 4 show large variations. Where both X-ray and DTA determinations were made on the same sample, the DTA temperature is considerably higher than the X-ray one, as observed by [2] and [25]. Thermoelectric power measurements, in addition to showing a peak at 112 °C, indicated some irregularity at around 125 °C and sometimes another maximum at 137 °C [26]. Similar irregularities also were observed in the X-ray and DTA results by [2] and [25] near the transformation temperatures. Such variations can arise if the composition shifts from stoichiometry to a two-phase region, for which the transformation temperature varies over a range of temperature. The magnitude of the transformation temperature in such situations also will be low because of its rapid fall at higher Se levels. Even if these facts can explain, in part, the discrepancies in the reported values in Table 4, the existence of a broad temperature range over which the $\alpha \rightarrow \beta$ transformation appears to take place cannot be discounted. This is supported by the observation of broad thermal effects [2, 25], anomalies in the conductivity and thermoelectric power [26, 29], and heat capacity variations over a large temperature interval, as observed by Kubaschewski and Nölting [30]. Thus, following [2], the $\alpha \rightarrow \beta$ transition temperature is taken over a 30 °C interval centered on 123 °C, i.e., at 123 ± 15 °C. A peritectoid transformation is consistent at this temperature with the existing phase boundaries, shown in Fig. 1 and 3, whereas both congruent and eutectoid transformations are unlikely under these conditions.

The reduction in the $\alpha \rightarrow \beta$ transformation temperature for the $Cu_{2-x}Se$ phase with increasing Se content is shown in Fig. 3, based on the DTA and conductivity results of [1] and [7], respectively. An invariant temperature at −103 °C was established by Ogorelec *et al.* [7], based on discontinuity in the electrical conductivity at that temperature for several Se alloys. The authors proposed the $\beta Cu_{2-x}Se$ to undergo a eutectoid (termed incorrectly as "eutectic") transformation at that temperature, forming $\alpha Cu_{2-x}Se$ as one of the products. In contrast, Stevels [25] still observed, in the $Cu_{1.86}Se$ alloy cooled to −170 °C, the presence of the fcc phase admixed with αCu_2Se. They also reported observing a superstructure of this phase below −115 °C.

$Cu_2Se/Cu_{2-x}Se$ Low-Temperature Phase. As noted earlier, the fcc $\beta Cu_2Se/\beta Cu_{2-x}Se$ undergoes polymorphic transformation at or below 123 ± 15 °C to form αCu_2Se. The $\alpha \rightleftarrows \beta$ transformation is reported to be sluggish [2]. Stevels *et al.* [11] obtained αCu_2Se mixed with the fcc phase in quenched samples (from 500 to 700 °C) of $Cu_{2-x}Se$, when $x < 0.15$. Possibly because of the slow kinetics of transformation, they failed to get a single-phase αCu_2Se even on slow cooling. The cell dimensions of αCu_2Se were found to vary little between the samples, which led them to conclude that the homogeneity range of αCu_2Se is very narrow at room temperature.

Ogorelec *et al.* [7, 27] indicate a narrow but finite width of the αCu_2Se phase field at room temperature and below, based on conductivity measurements. This suggests the occurrence of the low temperature form of the Cu-deficient $\alpha Cu_{2-x}Se$ compound.

Table 4 $\alpha \rightleftarrows \beta$ Transformation Temperature of $Cu_{2-x}Se$

Reference	Temperature, °C Method of measurement DTA(a)	X-ray	EC and TEP(b)
[1]	131(c)	···	···
[2]	136(d), 134(c)	123 ± 3	···
[3]	162(d)	···	···
[5]	143(d), 130(c)(e)	···	···
[18, 20]	···	<103	···
[11, 25]	~100(f)	80(d)	···
[26]	···	···	112
[27]	···	···	142
[28]	135(d)	···	···

(a) DTA, differential thermal analysis. (b) EC and TEP, electrical conductivity and thermoelectric power. (c) Cooling cycle. (d) Heating cycle. (e) Date for heating and cooling cycles shown reversed from those given by [5] to avoid contradiction. (f) Approximation between 90 °C for $Cu_{1.95}Se$ and 110 °C for $Cu_{2.0}Se$.

Cu_3Se_2 is formed by peritectoid reaction between $\beta Cu_{2-x}Se$ and $\beta CuSe$. The rate of this solid state reaction is exceedingly slow below 135 °C. This is supported by [14], who did not succeed in synthesizing a single-phase alloy with this structure. According to [1], quenching specimens with this composition from 360 °C often yielded large amounts of Cu_2Se_2 with only traces of other adjacent equilibrium compounds. This was contradicted by Stevels *et al.* [11], who succeeded in forming Cu_3Se_2 only on prolonged annealing (3 months) at 120 °C. Samples cooled slowly through the transformation temperature often contained only traces of Cu_3Se_2, and the reaction was not complete at room temperature even after several years. However, the transformation was found to be considerably enhanced by pressure or by shear and could be brought to completion by prolonged grinding of the specimen [2].

The reverse reaction of disproportionation of Cu_3Se_2 to its constituents is also very slow, but relatively faster than the formation reaction. Consequently, for transformation temperature determination, disproportionation reaction is utilized. Stevels [25] observed this temperature to differ between the X-ray and DTA methods, being 120 and 135 °C, respectively. Other reported temperatures based on DTA are 135 °C [1], 175 °C [3], 143 °C [5] and 112 °C [2]. A strong dependence of the result on heating rate was observed by [2], who obtained the values 131, 125 and 112 °C, corresponding to the heating rates 10 and 5 °C per minute and 8 °C per hour, respectively. The temperature, 112 °C, from the slowest heating rate measurement, approximated best the equilibrium condition and hence is accepted. The

compound is stable at room temperature to at least 35 kbar pressure [2].

CuSe is formed by peritectic reaction between $\beta Cu_{2-x}Se$ and Se-rich liquid. The measured peritectic temperatures are 400 °C [3], 387 ± 5 °C [4], 384 °C [5], 382 °C [1] and 377 °C [2]. The formation reaction was noted to be slower than the reverse disproportionation reaction [25].

The room temperature form of this phase, αCuSe, undergoes rapid polymorphic transformation to βCuSe at temperatures reported variously at 80 °C [3], 60 °C [5], 48 °C (by DTA, 46 °C by X-ray) [25], 53 °C [1] and 51 °C [2].

At still higher temperatures, a further polymorphic transformation from βCuSe to γCuSe was detected in the high-temperature X-ray by Stevels *et al.* [11]. Because no discontinuous change in enthalpy was detected in the $\beta \rightarrow \gamma$ transformation by the DTA method, the transformation is continuous, i.e., higher order. The $\beta \rightarrow \gamma$ transformation temperature observed by [11] is 120 °C, confirmed subsequently by [2]. Both $\alpha \rightarrow \beta$ and $\beta \rightarrow \gamma$ transformations are rapidly reversible [2].

The αCuSe is reported to be sensitive to pressure. Grinding in a mortar and pestle causes it to undergo disproportionation or possible transformation. Between 5 and 10 kbar, αCuSe disproportionates to Cu_3Se_2 and $CuSe_2$II (a form of $CuSe_2$ stabilized under pressure at <5 kbar) [2]. The peritectic decomposition temperature of γCuSe remains unaltered up to 5 to 6 kbar pressure. All transformation temperatures associated with CuSe are accepted from [2] for reasons explained earlier.

$CuSe_2$. Although Babitsyna *et al.* [3] denied the occurrence of $CuSe_2$, evidence in favor of its existence in the equilibrium diagram is overwhelming [1, 2, 11, 31, 32]. The compound is formed by peritectic reaction between γCuSe and the Se-rich liquid. The formation reaction is very slow, whereas the reverse disproportionation reaction is relatively rapid.

The measured peritectic temperature is given as ~340 °C [11], 343 °C [5], 342 °C [1] and 332 °C [2]. The representative temperature is accepted from [2].

According to Murray and Heyding [2], a cubic modification, $CuSe_2$II, having the pyrite-type structure is formed under pressure and on high-temperature annealing. This modification is reported to be more stable against decomposition than $CuSe_2$ at atmospheric pressure. $CuSe_2$II melts congruently at 545 °C under a pressure of 20 kbar [2].

Bither *et al.* [32] pioneered the high-pressure synthesis of $CuSe_2$ compound with the pyrite-type structures that are known to be superconductors below 2.4 K.

Metastable Phase

No metastable phase has been observed in the bulk prepared sample. However, in thin-film preparations several metastable phases have been noted. Boettcher *et al.* [33] observed, in thin films of $Cu_{1.8}Se$, seven distinct electron diffraction patterns between 20 and 320 °C, representing either body-centered cubic or tetragonal structure with different lattice parameters.

On vacuum thermal treatment of thin films (35 to 40 nm) of CuSe above 350 °C, Shafizade *et al.* [34]

Table 5 Crystal Structures

Phase	Approximate composition(a), at.% Se	Pearson symbol or structure	Prototype	Space group	Lattice parameters, nm a	b	c	Comment	Reference
(Cu)	~0	$cF4$	Cu	$Fm3m$	0.36147	···	···	At 18 °C, 0% Se	(b)
$\alpha Cu_{2-x}Se$	~33.3 to 33.8	Monoclinic	···	···	1.4087	2.0481	0.4145	β = 90° 23'; at 25 °C	[2]
$\beta Cu_{2-x}Se$	~33.3 to 36.4(c)	$cF12$	CaF_2	$Fm3m$[39]	0.5860	···	···	For x = 0	[35]
					0.5765	···	···	For x = 0.2 at 25 °C	[2]
Cu_3Se_2	40	Tetragonal	(Umangite)	$P\bar{4}2_1m$[41]	0.6385	···	0.4271	···	···
									[2]
αCuSe	50	Hexagonal	(Klockmannite)	$P6_3/mmc$[42]	0.3938	···	1.726	At 20 °C	[11]
βCuSe	50	Orthorhombic	···	···	0.3948	0.6958	1.7239	At 51 °C	[2]
γCuSe	50	Hexagonal	···	$P6_3/mmc$[39]	0.3984	···	1.7288	At 157 °C	[2]
$CuSe_2$	66.7	$oP6$	FeS_2	$Pnnm$[39]	0.50046	0.61822	0.37397	At 25 °C	[2]
(Se)	~100	$hP3$	Se	$P3_121$[Pearson]	0.4366	···	0.4958	100% Se	[36]

(a) From the phase diagram. (b) From Landolt-Börnstein. (c) Homogeneity range at room temperature, $0.18 \leq x \leq 0.22$ and at 500 °C, x = 0 to ~0.26.

Table 6 Lattice Parameters of αCu_2Se

Crystal structure	Lattice parameters, nm a	b	c	Temperature, °C	Comment	Reference
Tetragonal	1.163	···	1.140	<131	···	[35]
Tetragonal	1.151	···	1.174	<103	(a)	[19]
Orthorhombic	0.4118	0.7032	2.0381	25	···	[11]
Orthorhombic	0.410	0.702	2.03	~170	···	[11]
Monoclinic	1.4087	2.0481	0.4145	···	(b)	[2]

(a) Approximate composition, 33.8 at.% Se. (b) β = 90°23'.

detected by electron diffraction the occurrence of an fcc phase of lattice parameter a = 0.563 nm, corresponding to the composition $Cu_{1+x}Se$ mixed with the equilibrium Cu_2Se phase. The phase was stable down to room temperature.

Crystal Structure and Lattice Parameters

The crystal structure and the representative lattice parameter data from selected works for the different phases are presented in Table 5. Controversies exist in some of the reported structures and space groups, for which references are quoted in Table 5 in appropriate places. For structural notation, Pearson's designation is followed. Where such information is lacking, the corresponding crystal structure/Bravais lattice type is indicated. Similarly, where the phase for which the structure prototype information is not available but is known to have mineral equivalents in nature, the latter is presented. Pertinent information and lattice parameter data on each phase from different known works are presented under individual phase headings that follow.

αCu_2Se. This low-temperature modification of Cu_2Se, stable at room temperature, exhibits a complex diffraction pattern presenting difficulty in identification. Borchert [19] and Junod [35] identified it with a tetragonal cell, while Stevels *et al.* [11] proposed an orthorhombic lattice. By careful high-temperature X-ray, Murray and Heyding [2] established the structure as monoclinic and inferred it to correspond to a simple monoclinic distortion of the orthorhombic cell proposed by [11]. The lattice parameter was found to increase for the partially oxidized Cu_2Se sample that corresponded to the composition of the Se-rich boundary of the phase [2]. The variously reported structure and lattice parameters for the phase are presented in Table 6. αCu_2Se structure is found to remain unchanged down to liquid nitrogen temperature [11].

Table 7 Lattice Parameter of βCu_2Se

Reference	Lattice parameter, nm a	Temperature, °C	Comment
[19]	0.5840	170	···
[20]	0.5740	25	On berzelianite mineral
[20]	0.5820	55	On synthetic Cu_2Se
[21]	0.5840	180	···
[35]	0.5860	···	···
[37]	0.5754 ± 0.0003	···	32.8 at.% Se

$\beta Cu_2Se / \beta Cu_{2-x}Se$. The high-temperature modification of Cu_2Se is face-centered cubic, CaF_2-type, with lattice parameters as shown in Table 5. Lattice parameter data reported from various works are presented in Table 7.

As described in the section entitled "Equilibrium Diagram", the homogeneity range of Cu_2Se extends above the stoichiometric ratio to higher Se concentrations, forming the $Cu_{2-x}Se$ compound with an extensive phase field at elevated temperatures. In the stoichiometric Cu_2Se structure, the Se atoms form an fcc sublattice, and the smaller metal atoms occupy the interstitial tetrahedral and octahedral sites in the subcell. The resultant atomic positions in the unit cell of the fcc Cu_2Se, according to [19], are shown in Table 8. Compared to the corresponding atomic positions for the prototype phase CaF_2 [Pearson], also shown in Table 8, the interstitial site occupancy in the βCu_2Se is not restricted to tetrahedral sites alone. The Cu atoms also occupy part of the 4 octahedral and 32 trigonal sites. The atomic arrangements studied by Rahlfs [21] did not include the octahedral coordination for the Cu sites.

Stevels and Jollinek [11] corroborated the findings of Borchert [19], and the positions of the Cu atoms according to their model based on the high-temperature form of $Cu_{1.8}Se$ with the space group $F\bar{4}3m$, given by [19], are presented in Table 9. However, the model used by Heyding and Murray [39] for the occupancy of sites corresponding to $Cu_{1.80}Se$ at room temperature is perhaps the most consistent one because, unlike the previous authors, no distinction is made between the 4(*c*) and 4(*d*) equivalent (tetrahedral) sites. The model is based on the space group similar to that of the prototype, CaF_2. The results presented in Table 9 show that 5.2 Cu atoms occupy the tetrahedral sites and the re-

Table 8 Atomic Positions in CaF_2 [Pearson] and Isostructural βCu_2Se [19]

Phase	Space group	Atoms	Atomic position: Point set[†]	Atomic position: Coordinates[‡]	Site designation
CaF_2	$Fm\bar{3}m$	4 Ca	4(*a*),$m\bar{3}m$	0,0,0 + face-center translations	fcc
		8 F	8(*c*),$\bar{4}3m$	1/4,1/4,1/4; 1/4,3/4,3/4; 3/4,1/4,3/4; 3/4,3/4,1/4; 3/4,3/4,3/4; 3/4,1/4,1/4; 1/4,3/4,1/4; 1/4,1/4,3/4	Tetrahedral
βCu_2Se	$F\bar{4}3m$	4 Se	4(*a*)	0,0,0 + face-center translations	fcc
		4 Cu	4(*c*)	1/4,1/4,1/4; 1/4,3/4,3/4; 3/4,1/4,3/4; 3/4,3/4,1/4	Tetrahedral
		4 Cu	4(*b*)	1/2,1/2,1/2; 1/2,0,0; 0,0,1/2; 0,1/2,0	Octahedral
		Random occupation	16(*e*)	(x,x,x); $(\bar{x},\bar{x},x)$	Trigonal x = 0.33 and x = 0.67 for 1/4 of these Cu
		0 Cu	4(*d*)	3/4,3/4,3/4; 3/4,1/4,1/4; 1/4,3/4,1/4; 1/4,1/4,3/4	Tetrahedral

(†) According to Wyckoff's notation, [38]. (‡) Coordinates in a particular set indicated by parentheses.

Table 9 Atomic Positions in $\beta Cu_{1.80}Se$ for Different Space Groups

Space group	Atoms	Atomic Position Point set	Coordinates†	Reference
$F\bar{4}3m$	4 Se	4(a)	0,0,0 + face-center translations	[11]
	0.6 Cu	4(b)	1/2,1/2,1/2; (1/2,0,0)	
	4 Cu	4(c)	(1/4,1/4,1/4)	
	2.6 Cu	16(e)	(x,x,x); $(x,\bar{x},\bar{x})$‡	
$Fm3m$	4 Se	4(a)	0,0,0 + face-center translations	[39]
	5.2 Cu	8(c)	(1/4,1/4,1/4); (3/4,3/4,3/4)	
	(Random)	...	(tetrahedral sites)	
	2 Cu	32(f)	± {(x,x,x); $(x,\bar{x},\bar{x})$ (trigonal sites)}	

(†) Coordinates in a particular set enclosed within parentheses. (‡) $x = 0.7$.

Table 10 Lattice Parameter of $\beta Cu_{2-x}Se$

Reference	Lattice parameter, nm a	Temperature, °C	Composition x	Composition at.% Se
[1]	0.57648 ± 0.0001	26	0.16	35.2
[1]	0.57594 ± 0.0001	26	0.20	35.7
[1]	0.5743 ± 0.0002	26	0.30	37.0
[2]	0.5765	25	0.20	35.7
[5]	0.57486 ± 0.00021	75	0.18	35.5
[5]	0.57387 ± 0.0002	75	0.22	36.0
[5]	0.57390 ± 0.00027	75	0.26	36.5
[5]	0.57499 ± 0.0001	75	0.14	35.0
[5]	0.57630 ± 0.0001	175	0.14	35.0(a)
[5]	0.57608 ± 0.0001	350	0.14	35.0(a)
[5]	0.57589 ± 0.00007	500	0.14	35.0(a)
[16]	0.5758	25	0.20	35.7
[19]	0.5729	...	0.20	35.7
[20]	0.575	25	0.15	35.1
[25]	0.5751	25	0.20	35.7
[25]	0.5780	150	0.20	35.7(a)
[25]	0.5842	200	0.20	35.7(a)
[25]	0.5904	320	0.20	35.7(a)
[40]	0.57605	25	0.20	35.7

(a) Tentative composition — actual composition probably is lower due to evaporation of Se.

maining 2 Cu atoms go to the trigonal sites; the octahedral sites remain unoccupied.

Nonoccupancy of part of the available (total 8) tetrahedral sites by Cu atoms indicates the existence of vacancy in Cu sites. Thus, $Cu_{2-x}Se$ is a vacancy compound. Apparently the Cu site vacancy persists even at stoichiometric composition, Cu_2Se, because all tetrahedral sites are still not occupied (Table 8) and, therefore, additional site vacancies also exist at trigonal and octahedral sites. Consequently, the $Cu_{2-x}Se$ compounds exhibit interesting electron transport properties that will be discussed later.

The lattice parameters of $\beta Cu_{2-x}Se$ vary with both composition and temperature, as demonstrated in the different works in Table 10. Often the effect of temperature is masked by the concomitant change in composition due to the rapid evaporation of Se from the alloy at high temperatures. The data of [25] and [5] supposedly show this combined effect. However, the lattice parameters in general decrease with the increase

Table 11 Lattice Parameters of Cu_3Se_2

Reference	Lattice parameters, nm a	c	Comment
[1]	0.6394 ± 0.0005	0.4269 ± 0.0005	...
[2]	0.6385	0.4271	...
[11]	0.6405	0.4278	At 20 °C
[11]	0.6428	0.4278	At 100 °C
[39]	0.64024	0.42786	For umangite mineral
[41]	0.6406	0.4279	...
[42]	0.6402	0.4276	...

Table 12 Lattice Parameters of αCuSe

Reference	Lattice parameters, nm a	c	Comment
[1]	0.3940 ± 0.0003	1.7216 ± 0.0005	...
[2, 39]	0.3934	1.7217	...
[11, 25](a)	0.3938	1.726	At 20 °C
[42]	0.3938	1.725	For klockmannite mineral
[43]	0.3940	1.725	...
[44]	0.3960	1.726	For vapor-deposited thin film
[45]	0.3940	1.728	For vapor-deposited thin film

(a) Report superstructure at 20 °C with $a = 1.420$ nm and $c = 1.726$ nm.

in Cu vacancy or, conversely, with the increase in Se content [1, 5]. The anomaly in the lattice parameters between 75 and 500 °C for $Cu_{1.86}Se$ given by [5] can be understood in terms of the normal thermal expansion of lattice with increasing temperature, as in 75 to 175 °C data, whereas, above this temperature, the lattice parameters decrease because of the compositional shift of the alloy to lower Se concentrations due to evaporation of Se.

Cu_3Se_2. Morimoto and Koto [41] determined the structure of Cu_3Se_2 as tetragonal with the space group $P\bar{4}2_1m$. Earlier, Berry [42] presented lattice parameters also based on the tetragonal unit cell but with a different space group. The lattice parameters from different works are shown in Table 11. The lattice parameters of the natural mineral umangite having the same composition [39] are slightly higher than the synthetic counterpart [2]. The orthorhombic structure with lattice parameters $a = 0.428$, $b = 0.640$ and $c = 1.247$ nm proposed by [20] is apparently incorrect.

αCuSe. Early [43] determined that the synthetically prepared room temperature form of CuSe, αCuSe, is similar in X-ray pattern with the mineral klockmannite (CuSe). He determined the lattice dimensions based on the hexagonal cell that agree closely with the analysis of Berry [42] on klockmannite, who determined also the atomic positions for the structure. These and other results are presented in Table 12. The lattice parameters by Stevels and Jellinek [11] on synthetic αCuSe at 20 °C agree closely with those of [42] and [43] and are taken as representative.

Superstructure reflections with 12-fold multiplicity of the a-axis were observed by [43]. This was confirmed subsequently by [11] on samples held at room temperature for several months and also by [46] and [47]. Heyding [2] did not notice extra reflection on freshly prepared samples but confirmed their appearance on long aging at room temperature, indicating a slow process of ordering. Taylor *et al.* [46] ascribed the ordering to twinning in the lattice and suggested a 13-fold multiplicity of the a-axis.

β CuSe has a c-end base-centered orthorhombic structure, for which lattice parameters are shown in Table 13. The results by Heyding [2], which show good agreement with those of [1] and [11], are accepted as representative values in Table 5.

γ CuSe possesses hexagonal symmetry, for which lattice dimensions are presented in Table 14. The diffraction patterns of α CuSe and γ CuSe are very similar in terms of both Miller indices and relative intensities of the X-ray lines. However, because the interplanar spacings have large differences, Heyding [2] considers the two

Table 13 Lattice Parameters of β CuSe

Reference	Lattice parameters, nm a	b	c	Comment
[1]	0.6813 ± 0.001	0.4015 ± 0.001	1.7095 ± 0.002	···
[2]	0.3948	0.6958	1.7239	At 51 °C
[11]	0.3949	0.6935	1.720	At 60 °C

Table 14 Lattice Parameters of γ CuSe

Reference	Lattice parameters, nm a	c	Comment
[2]	0.3984	1.7288	At 157 °C
[11]	0.3976	1.7243	At 140 °C

Table 15 Lattice Parameters of $CuSe_2$

Reference	Lattice parameters, nm a	b	c	Comment
[1]	0.5017 ± 0.001	0.6198 ± 0.001	0.3741 ± 0.0005	···
[2]	0.50046	0.61822	0.37397	At 25 °C
[11]	0.6196	0.5020	0.3741	At 25 °C
[39]	0.5005	0.6182	0.3740	···
[48]	0.5103	0.6292	0.3817	···

polymorphs not isostructural. The lattice parameter result of [2] is accepted as representative of the system and is shown in Table 5.

$CuSe_2$ has orthorhombic, $C17$ marcasite-type structure. The atom positions and the structure were determined by Gattow [48]. The lattice parameters determined by several authors are given in Table 15. Accepted values are taken from [2] and shown in Table 5. The lattice parameter for the high-pressure modification of $CuSe_2$ having the cubic pyrite-type structure is $a = 0.6116$ nm at room temperature [2].

Thermodynamics

The heats (enthalpies) of formation of the different Cu-Se compounds from various works are presented in Table 16. The corresponding standard entropy of formation (at 25 °C) results are presented in Table 17. The heats of formation data refer to 25 °C except where indicated otherwise.

In general, fair agreement is shown between the different works in the values of ΔH and, to a lesser extent, in the values of S°_{298}. The S°_{298} value for $Cu_{1.75}Se$ by [49] appears to be too high, and the ΔH values for Cu_2Se and the four $Cu_{2-x}Se$ compounds by [50] are considerably lower than the other reported values. The ΔH values calculated from thermal analysis data by [1] are in considerable discord with other literature values and are not included in the tables.

The heat capacity data for αCu_2Se and βCu_2Se given by [30] are as follows:

αCu_2Se: 58.6 + 77.4 T (J/mol deg)	(298 to 395 K)
βCu_2Se: 84.1 (J/mol deg)	(395 to 800 K)

Addendum

Special Properties

$Cu_{2-x}Se$ is a p-type semiconductor with a carrier concentration of $\approx 10^{19}$ cm^{-3} and band gap between 1.1 and 1.7 eV [53, 54]. The electronic transport properties are characterized by positive signs of the thermal emf and the Hall constant and by the negative temperature coefficient of electrical resistivity in certain temperature ranges [55, 56].

Apparently, the semiconductor type of properties results from the defect structure of $Cu_{2-x}Se$ arising from

Table 16 Heats of Formation of Cu-Se Compounds

Compound	Heats of formation, $-\Delta H^\circ$ (kJ/mol) from reference [31](a)	[49](b)	[50](c)	[51](d)	[52]	[2](e)
$CuSe_2$	43.1	49.0	···	39.3 ± 3.3	···	40.2 ± 16.7
CuSe	39.6	44.0 ± 4.2	···	32.6 ± 3.3	41.9 ± 4.2	···
Cu_3Se_2	98.9	···	···	94.6 ± 10.5	···	41.9 ± 20.9
Cu_2Se	54.5	62.8 ± 4.2	21.8 ± 0.6	65.7 ± 6.3	···	26.8 ± 8.4
$Cu_{2-x}Se$	···	···	···	···	65.3 ± 6.3(f)	···
$Cu_{1.95}Se$	···	···	22.1 ± 0.8	···	···	···
$Cu_{1.90}Se$	···	···	24.8 ± 0.8	···	···	···
$Cu_{1.85}Se$	···	···	32.6 ± 0.8	···	···	···
$Cu_{1.80}Se$	55.4	···	33.4 ± 0.8	···	···	···

(a) By direct calorimetric method; at 25 °C. (b) By vapor pressure method; at 25 °C. (c) By isoperibol liquid metal (Bi) solution calorimetric method; at 352 °C. (d) By emf method; at 25 °C. (e) From area of thermal analysis peak; at respective transformation temperatures. (f) $x = 0.333$ to 0.358; at 25 °C.

Table 17 Standard Entropy of Cu-Se Compounds

Compound	Entropy, S°_{298} (J/mol/deg) from reference [49]	[51]	[52]
$CuSe_2$	120.6	98.8 ± 5.0	...
CuSe	86.2	74.1 ± 4.2	71.6 ± 12.6
Cu_2Se_3	...	185.0 ± 8.4	207.2 ± 20.9
$Cu_{2-x}Se$	595.2(a)	...	129.8 ± 4.2(b)
Cu_2Se	162.4	80.4 ± 5.4	113.9
	157.4	...	...

(a) For $x = 0.25$. (b) For $x = 0.333$ to 0.355.

the occurrence of vacancies in the Cu site, whose formation energy is characteristically low [56]. The copper vacancies supposedly create low-lying accepter levels in the band gap that are occupied at ordinary temperatures, and the resultant holes in the valence band account for the hole conduction. Sorokin *et al.* [56] observed, for composition changes from Cu_2Se to $Cu_{1.81}Se$, a progressive change in the lattice parameter from 0.578 to 0.568 nm and in the density from 7.10 to 6.72 g/cm^3, which was attributed to the formation of the copper-deficient structures. The corresponding changes in the electrical conductivity (σ), Hall constant (R), thermoelectric coefficient (α), carrier concentration (n) and carrier mobility (μ) were from 85 to 6200 Ω^{-1}cm^{-1}, 19.7 to 1.40×10^{-3} cm^3/°C, 472 to 20 μV/deg, 2.76×10^{17} to 5.26×10^{21} cm^{-3} and 1420 to 7.35 cm^2/V s, respectively. For the stoichiometric composition, Cu_2Se, the transport properties showed extreme sensitivity to the purity of the starting material, whereas this was not so for the defect structures. Thus, for example, σ changed from 480 to 2250 for $Cu_{1.98}Se$ and from 3060 to 3080 Ω^{-1}cm^{-1} for $Cu_{1.93}Se$, corresponding to spectral pure starting material and for 99.92 Cu and 99.96 Se, respectively, showing the strong doping effect of impurities characteristic of an extrinsic semiconductor.

In $Cu_{2-x}Se$, the carrier concentration increases with the progressive increase in copper deficiency, and the conductivity also increases correspondingly. The highest value is reported to be reached at composition similar to berzelianite ($\sigma = 6000\ \Omega^{-1}$cm^{-1}). Over wide temperature ranges, $Cu_{2-x}Se$ exhibits metallic-type conductivity but, according to Abdulliev *et al.* [57], a transition to semiconductor-type characteristic with a negative temperature coefficient of resistivity occurs around 600 °C, depending on composition. Similar behavior is also reported to be exhibited between 20 to 50 °C.

$CuSe_2$ with pyrite-type structure is a superconductor, with the critical temperature between 2.30 and 2.43 K [32]. Bither *et al.* [32] synthesized this structure from stoichiometric mixtures under high pressure (65 kbar) and high temperature (1000 to 2000 °C). For a lower synthesis temperature (900 °C), the pyrite structure was found by Krill *et al.* [58] to be stable over a narrow composition range around the stoichiometry, and to undergo a weak ferromagnetic transition at a lower temperature (31 K) before turning into a superconductor. The superconducting critical temperature, however, remains unchanged in both instances.

Cited References

1. R. D. Heyding, *Can. J. Chem.*, *44*(10), p 1233-1236 (1966).
2. R. M. Murray and R. D. Heyding, *Can. J. Chem.*, *53*(6), p 878-887 (1975).
3. A. A. Babitsyna, T. A. Emelyanova, M. A. Chernitsyna and V. T. Kalinnikov, *Zh. Neorg. Khim.*, *20*(11), p 3093-3096 (1975) in Russian; translated as *Russ. J. Inorg. Chem.*, *20*(11), p 1711-1713 (1975).
4. G. P. Bernardini and A. Catani, *Miner. Deposita* (Berl.), *3*(4), p 375-380 (1968).
5. G. P. Bernardini, F. Corsini and R. Trosti, *Period. Miner.*, *41*(3), p 565-586 (1972) in Italian.
6. B. P. Burylev, N. N. Fedorova and L. Sh. Tsemekhman, *Zh. Neorg. Khim.*, *19*(8), p 2283-2285 (1974) in Russian; translated as *Russ. J. Inorg. Chem.*, *19*(8), p 1249-1250 (1974).
7. Z. Ogorelec, B. Mestnik, D. Devčić, *J. Mater. Sci.*, *7*(8), p 967-969 (1972).
8. D. R. Mason and D. F. O'Kane, International Conference on Semiconductor Physics, Prague, 1960, Academic Press, NY, p 1026-1031 (1961).
9. K. Dies, *Kupfer und Kupferlegierungen in der Technik*, Springer, Berlin (1967) quoted by [4].
10. *Bull. Alloy Phase Diagrams*, *2*(1), p 146 (1981) quoting melting points of elements with corrections to conform to the 1968 temperature scale.
11. A. L. N. Stevels and J. Jellinek, *Rec. Trav. Chim.*, *90*, p 273-283 (1971).
12. P. L. Tayler, D. L. Wagoner and C. H. Pitt, *Met. Trans.*, *7B*, p 103-106 (1976).
13. J. S. Smart and A. A. Smith, *Trans. AIME*, *166*, p 144-155 (1946).
14. W. Borchert and I. Patzak, *Heidelb. Beitr. Min. Petr.*, *4*, p 434-442 (1955).
15. A. D. Bigvava, A. P. Zhirnova, R. R. Shvangiradze and P. G. Yudin, *Izv. Akad. Nauk SSSR Neorg. Mater.*, *16*(7), p 1292-1295 (1980) in Russian.
16. V. N. Konev and V. A. Kudinova, *Izv. Akad. Nauk SSSR Neorg. Mater.*, *9*(7), p 1132-1137 (1973) in Russian; translated as *Inorg. Mater.*, *9*(7), p 1008-1011 (1973).
17. R. de Medicis, thesis, Louvain (1967) quoted by [11].
18. G. Lorenz and C. Wagner, *J. Chem. Phys.*, *26*, p 1607-1608 (1957).
19. W. Borchert, *Z. Krist.*, *106*, p 5-24 (1945).
20. J. W. Early, *Am. Miner.*, *35*, p 337-364 (1950).
21. P. Rahlfs, *Z. Phys. Chem.*, *B31*, p 157-194 (1936).
22. V. N. Konev and V. A. Kudinova, *Izv. Akad. Nauk SSSR Neorg. Mater.*, *11*(7), p 1318-1319 (1975) in Russian; translated as *Inorg. Mater.*, *11*(7), p 1124-1126 (1975).
23. V. N. Konev, P. N. Inglizyan, S. A. Fomenkov, V. M. Berezin and V. A. Mezrin, *Izv. Akad. Nauk SSSR Neorg. Mater.*, *16*(10), p 1750-1752 (1980) in Russian; translated as *Inorg. Mater.*, *16*(10), p 1185-1187 (1980).
24. S. Migatanai and T. Ishikawa, *J. Phys. Soc. Jpn.*, *42*, p 159 (1977).
25. A. L. N. Stevels, *Philips Res. Rep. Suppl.*, No. 9, p 1-124 (1969).
26. Z. Ogorelec and B. Celustka, *J. Phys. Chem. Sol.*, *27*, p 615-617 (1966).
27. Z. Ogorelec and B. Celustka, *J. Phys. Chem. Sol.*, *30*, p 149-155 (1969).
28. J. B. Clark and E. Rapoport, *J. Phys. Chem. Sol.*, *31*, p 247-254 (1970).
29. R. Routie, M. Sudres and J. Mahenc, *J. Electroanal. Chem.*, *25*, p 489-496 (1970); *J. Chim. Phys.*, *67*, p 1013-1017 (1970).
30. P. Kubaschewski and N. Nölting, *Ber. Busenges. Physik. Chem.*, *77*(2), p 70 (1973).
31. G. Gattow and A. Schneidener, *Z. Anorg. Allgem. Chem.*, *286*, p 296-306 (1956).
32. T. A. Bither, C. A. Prewitt, J. L. Gillson, P. E. Bierstedt, R. B. Flippen and H. S. Young, *Solid State Commun.*, *4*, p 533-535 (1966).

33. A. Boettcher, G. Haase and H. Treupel, *Z. Angew. Phys.*, *7*, p 478-487 (1955).
34. R.B. Shafizade, I.V. Ivanova and M.M. Kazinets, *Thin Solid Films*, *55*, p 211-220 (1978).
35. P. Junod, *Helv. Phys. Acta*, *32*, p 567-600 (1959).
36. J. Donohue, *The Structure of the Elements*, John Wiley, NY (1974).
37. R.G. Azerbaeva, O.F. Kuchanskaya and V.D. Melikhov, *Vestn. Akad. Nauk Kaz. SSR*, *18*(9), p 34-43 (1962) in Russian.
38. R.W.G. Wyckoff, *Crystal Structures*, 2nd ed., Vol. 1, Interscience Publ., NY (1963).
39. R.D. Heyding and R.M. Murray, *Can. J. Chem.*, *54*(6), p 841-848 (1976).
40. A. Tonejc, Z. Ogorelec and B. Mestnik, *J. Appl. Cryst.*, *8*, p 375-379 (1975).
41. N. Morimoto and K. Koto, *Science*, *152*, p 345 (1966).
42. L.G. Berry, *Amer. Miner.*, *39*, p 504-509 (1954).
43. J.W. Early, *Amer. Miner.*, *34*, p 435-440 (1949).
44. L.G. Berry and R.M. Thomson, *Geol. Soc. Amer. Mem.*, *85*, p 43 (1962).
45. A. Singh, O.N. Srivastava and B. Dayal, *Acta Cryst.*, *B28*, p 635-638 (1972).
46. C.A. Taylor and F.A. Underwood, *Acta Cryst.*, *13*, p 361-362 (1960).
47. J.A. Elliott, J.A. Bicknell and R.G. Collinge, *Acta Cryst.*, *B25*, p 2420 (1969).
48. G. Gattow, *Z. Anorg. Allgem. Chem.*, *340*, p 312-318 (1965).
49. H. Rau and A. Rabenau, *J. Sol. State Chem.*, *1*(3-4), p 515-518 (1970).
50. K.G. Skeoch and R.D. Heyding, *Can. J. Chem.*, *51*, p 1235-1238 (1973).
51. K.A. Askerova, N.A. Alieva, T.Kh. Azizov, A.S. Abbasov and F.M. Mustafayev, *Izv. Akad. Nauk Azerb SSR*, *6*, p 137-139 (1976) in Russian.
52. K.C. Mills, *Thermodynamic Data for Inorganic Sulphides, Selenides and Tellurides*, Butterworth, London (1974).
53. G. Sorokin, Yu. Papshev and P. Oush, *Fiz. Tverd. Tela*, *7*, p 2244-2245 (1965) in Russian; translated as *Sov. Phys. Solid St.*, *7*, p 1810-1811 (1965).
54. G. Sorokin, *Izv. Vyssh. Uchebn. Zaved. Fiz.*, *6*, p 158 (1961) in Russian.
55. G.A. Efendiev, M.Ya. Bakirov and E.S. Zaidova, *Izv. Akad. Nauk SSSR Neorg. Mater.*, *5*(8), p 1460-1461 (1969) in Russian; translated as *Inorg. Mater.*, *5*(8), p 1244-1245 (1969).
56. G.P. Sorokin, G.Z. Idrichan, L.V. Dergach, E.V. Kovtun and Z.M. Sorokina, *Izv. Akad. Nauk SSSR Neorg. Mater.*, *10*(6), p 969-974 (1974) in Russian; translated as *Inorg. Mater.*, *10*(6), p 834-838 (1974).
57. B. Abdulliev, L.A. Aliyarova and G.A. Asadov, *Phys. Stat. Solidi*, *21*, p 461-464 (1967).
58. G. Krill, P. Panissod, M.F. Lapierre, F. Gautier, C. Robert and M.N. Eddine, *J. Phys. C*, *9*, p 1521-1533 (1976).

Cu-Se evaluation contributed by **D.J. Chakrabarti** and **D.E. Laughlin**, Department of Metallurgical Engineering and Materials Science, Carnegie-Mellon University, Pittsburgh, PA 15213, USA. Work was supported by the International Copper Research Association, Inc., (INCRA) and the Department of Energy through the Joint Program on Critical Compilation of Physical and Chemical Data coordinated through the Office of Standard Reference Data (OSRD), National Bureau of Standards. Literature searched through 1980. Prof. Laughlin is the ASM/NBS Data Program's Category Editor for binary copper alloys.